

Electromagnetic fields in small systems from AMPT

Xin-Li Zhao(赵新丽)

Collaborators: Yu-Gang Ma (马余刚), Guo-liang Ma (马国亮)

Workshop on AMPT, 四川大学

2017.7.26



中国科学院上海应用物理研究所
Shanghai Institute of Applied Physics, Chinese Academy of Sciences

outline

1 Introduction

① Heavy-Ion Collisions

② CME

③ $\langle \cos 2(\Psi_B - \Psi_2) \rangle$

④ AMPT model

2 Numerical results & discussions

① *EM* fields in *AuAu*, *PbPb* collisions

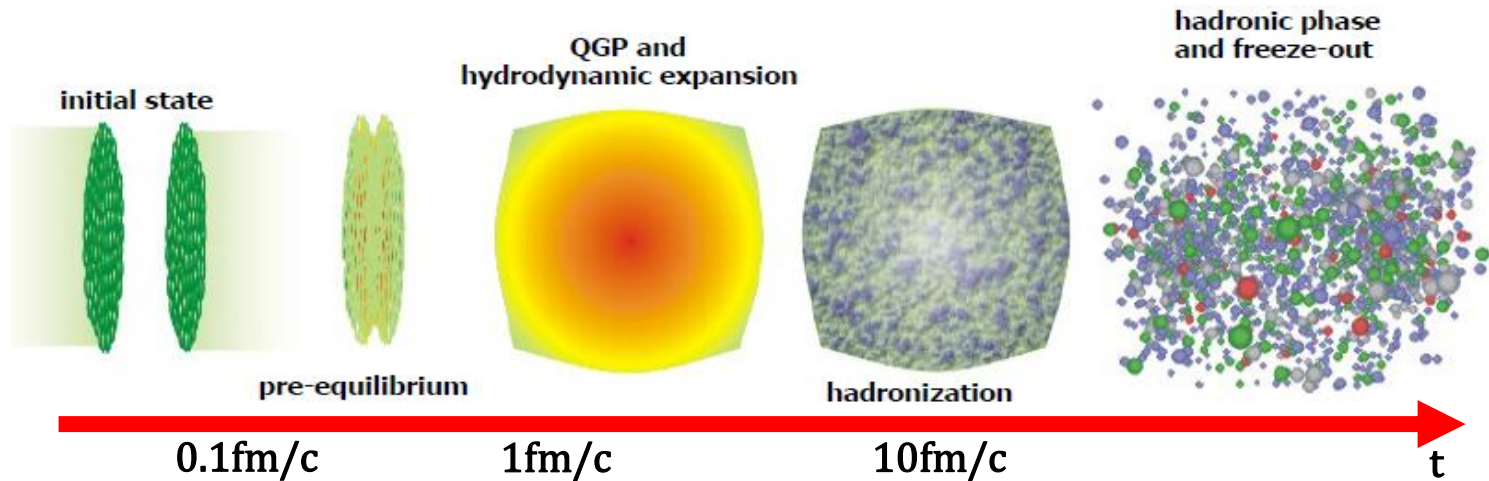
② *EM* fields in *pAu*, *dAu*, *pPb* collisions

③ Spatial distribution of *EM* fields in *pPb* collisions

④ $\langle \cos 2(\Psi_B - \Psi_2) \rangle$ in *pAu*, *dAu*, *pPb* collisions

3 Summary

Introduction: Space-Time Evolution for Heavy-Ion collisions



- The **pre-equilibrium** phase occurs at $t < 1 \text{ fm}/c$, during which cascades occur between partons, and a large number of quarks are generated.
- The system quickly reaches the **local thermal equilibrium** and then enters the **hydrodynamic expansion** stage at $1-10 \text{ fm}/c$.
- The temperature of the system decreases and begins to enter the **hadronization**. When there is no inelastic scattering between the hadrons, the **chemical equilibrium** is reached.
- After the chemical equilibrium, the system will continue the elastic scattering for some time, and finally when the elastic scattering between the hadrons are stopped, it is called the **kinetic freeze-out** stage.

Introduction: Magnetic fields



The Earth's magnetic field

0.6 Gauss

A common, hand-held magnet

100 Gauss

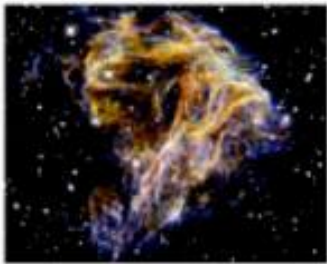


The strongest steady magnetic fields achieved so far in the laboratory

4.5×10^5 Gauss

The strongest man-made fields ever achieved, if only briefly

10^7 Gauss

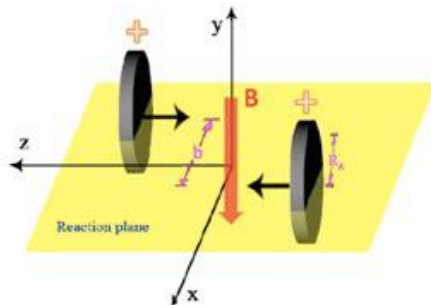


Typical surface, polar magnetic fields of radio pulsars

10^{13} Gauss

Surface field of Magnetars

10^{15} Gauss



The B field at the colliding time $t=0$. Biot-Savart law :

$$-eB_y \sim 2 \times \gamma \frac{e^2}{4\pi} Z v_z \left(\frac{2}{b}\right)^2 \sim \mathbf{10^{18} Gauss}$$

Introduction: Formulas of EM fields

According to Liénard-Wiechert potentials:

$$\phi = \frac{q}{4\pi\epsilon_0[r-(\mathbf{v}/c)\cdot\mathbf{r}]}$$

$$\mathbf{A} = \frac{q\mathbf{v}}{4\pi\epsilon_0c^2[r-(\mathbf{v}/c)\cdot\mathbf{r}]}$$

We can get the formulas of EM fields:

$$e\mathbf{E}(t, \mathbf{r}) = \frac{Ze^2}{4\pi\epsilon_0} \sum_n \frac{\mathbf{R}_n - R_n\mathbf{v}_n}{(R_n - \mathbf{R}_n \cdot \mathbf{v}_n)^3} (1 - v_n^2)$$

$$e\mathbf{B}(t, \mathbf{r}) = \frac{Ze^2}{4\pi\epsilon_0c} \sum_n \frac{\mathbf{v}_n \times \mathbf{R}_n}{(R_n - \mathbf{R}_n \cdot \mathbf{v}_n)^3} (1 - v_n^2)$$

Here $t=0$, \mathbf{r} is the center of mass of participants.

Introduction: Chiral Magnetic Effect

spin alignment in B-field:
opposite directions for
opposite charges

chirality

left

right

handedness:
momentum and spin,
aligned or anti-aligned



+

charge



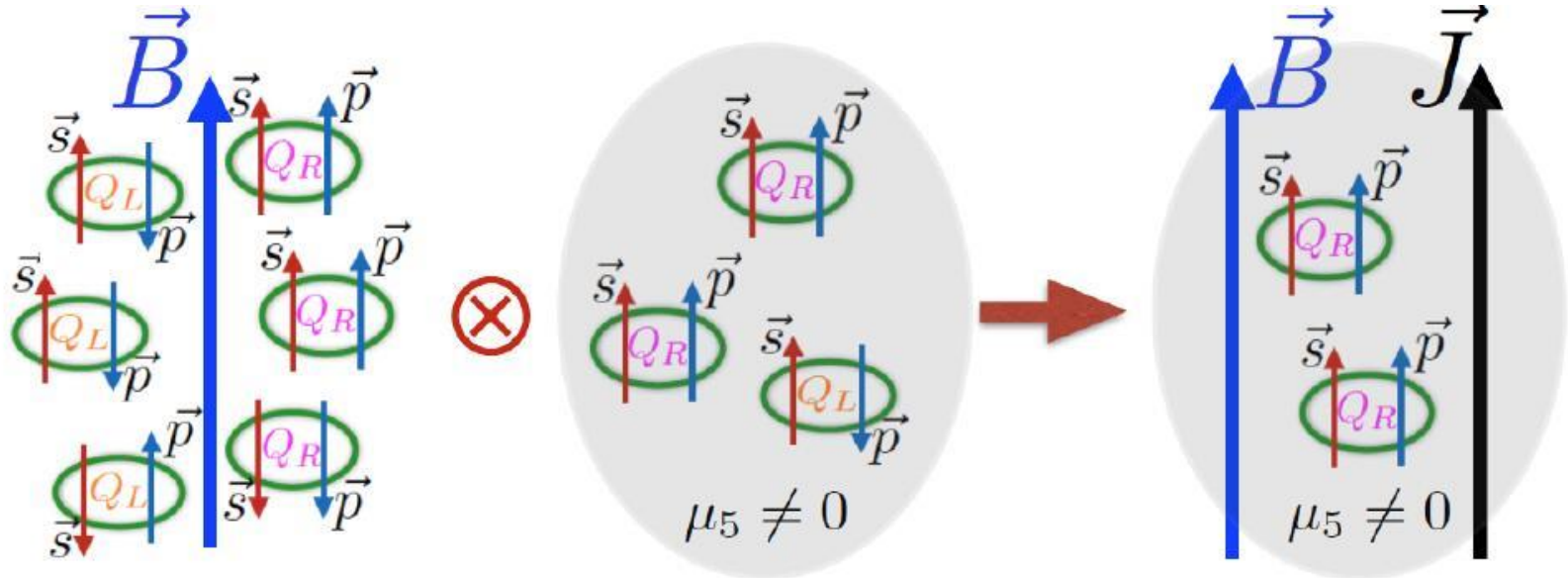
-

negative goes up
positive goes down

positive goes up
negative goes down

courtesy of P.Sorensen

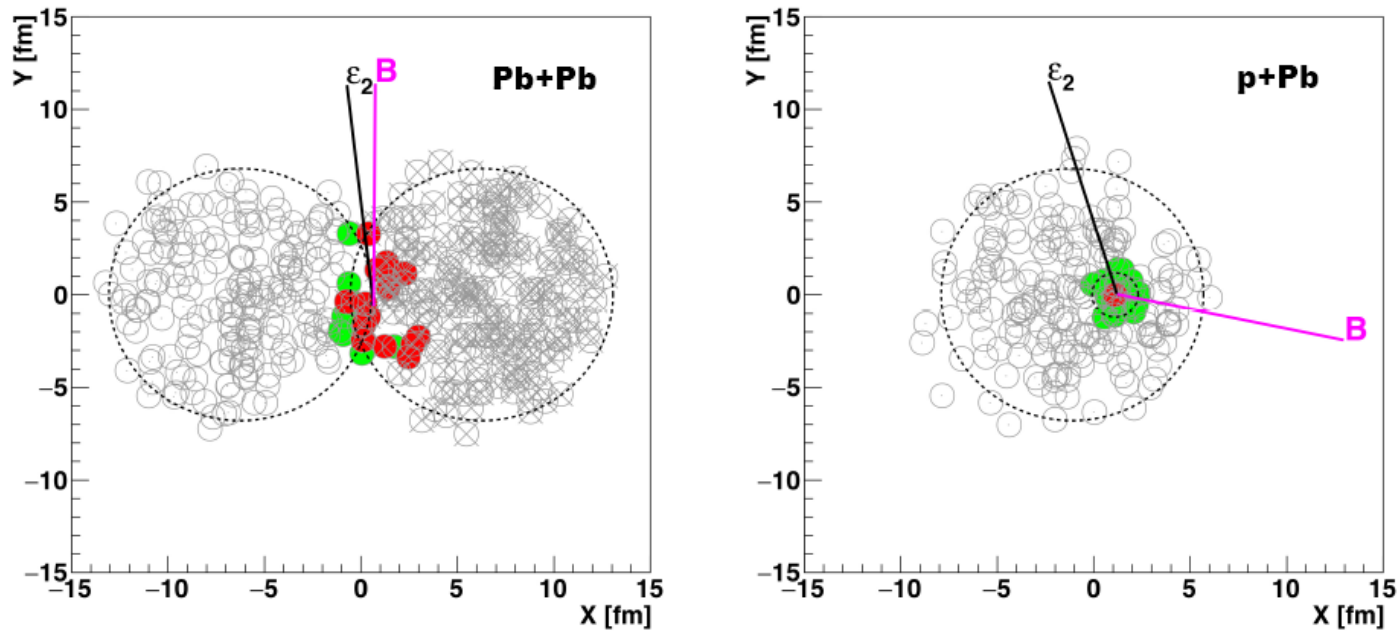
Introduction: Chiral Magnetic Effect



The chiral anomaly of QCD creates differences in the number of left and right handed quarks. An excess of right or left handed quarks lead to a current flow along the magnetic field.

$$\vec{J} = \frac{e^2}{2\pi^2} \mu_5 \vec{B}$$

Introduction: to be CME or not to be CME ?

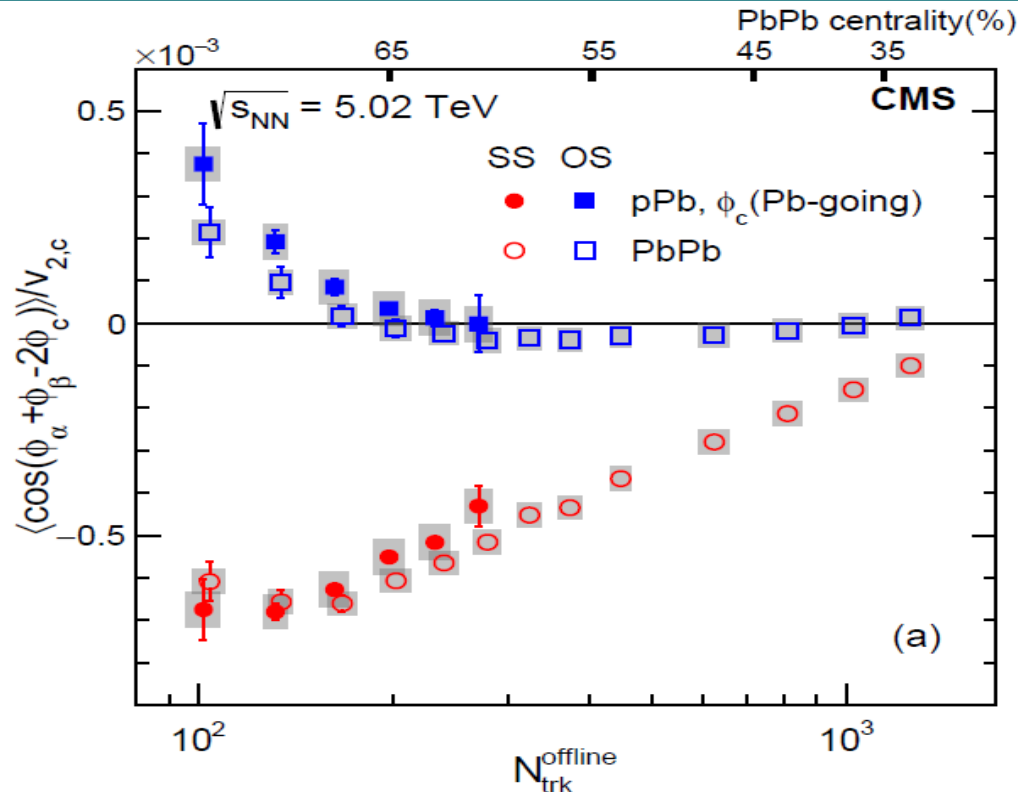


R. Belmont and J.L. Nagle, arXiv:1610.07964v1

$Pb + Pb: \epsilon_2 \parallel \Psi_B$

$p + Pb: \epsilon_2 \text{ is random}$

Introduction: to be CME or not to be CME ?



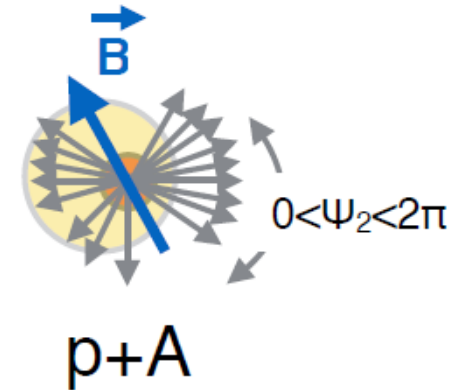
V. Khachatryan et al. (CMS), (2016), arXiv:1610.00263 [nucl-ex].

Similar magnitude and multiplicity dependence of the three-particle correlator observable in pPb collisions relative to that in PbPb collisions indicates that the dominant contribution of the correlation signal may not be related to the CME.

Introduction : Ψ_B and Ψ_2

Charge separation signal: $\Delta r \propto \langle B^2 \cos 2(\Psi_B - \Psi_{EP}) \rangle$

In pA collisions, if $\langle \cos 2(\Psi_B - \Psi_{EP}) \rangle \approx 0 \Rightarrow \Delta r^{CME} \approx 0$

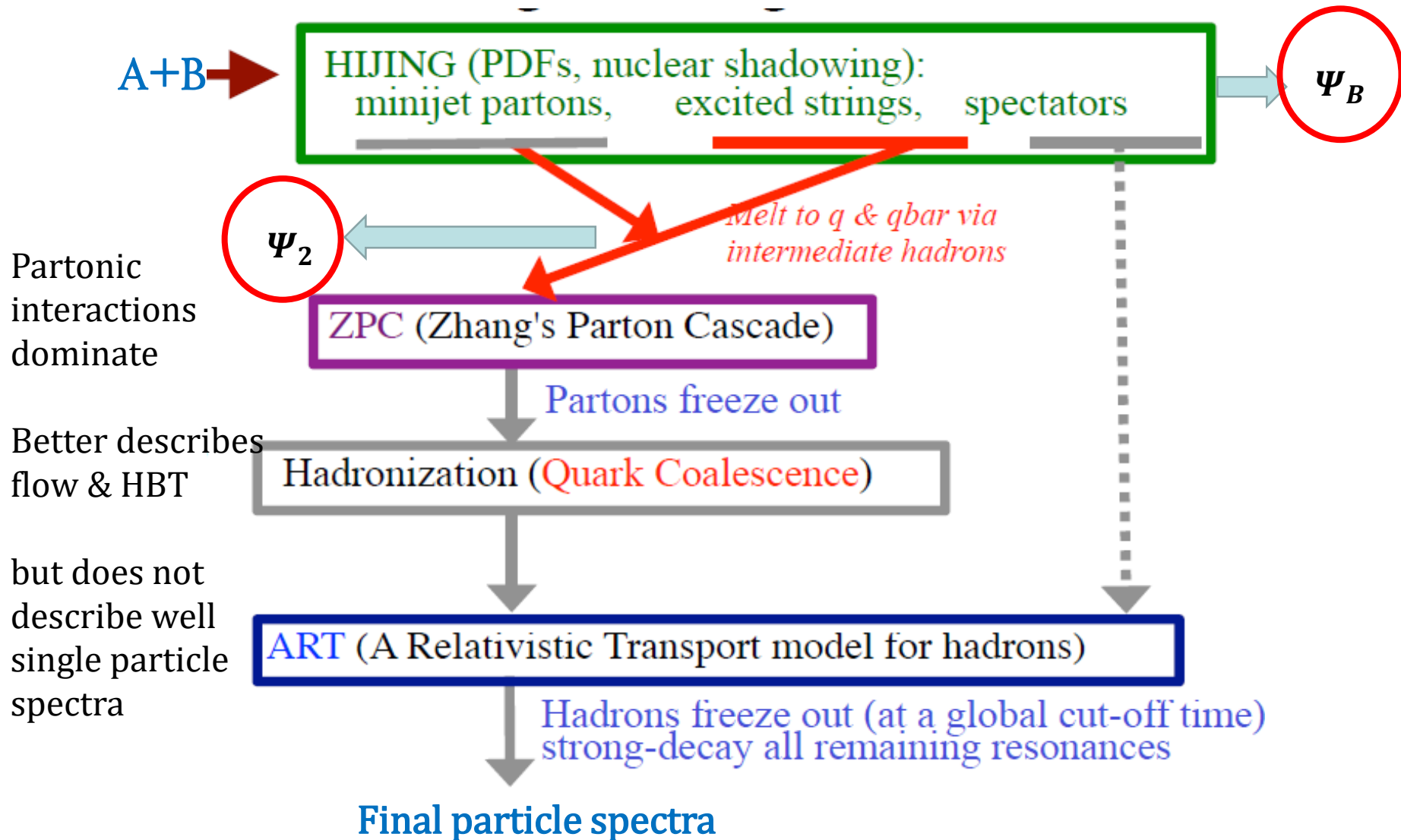


Our work: ① magnetic field

② $\langle \cos 2(\Psi_B - \Psi_2) \rangle$

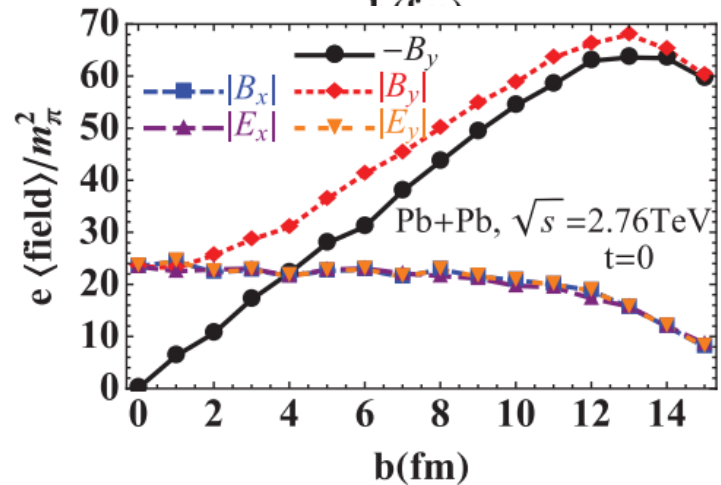
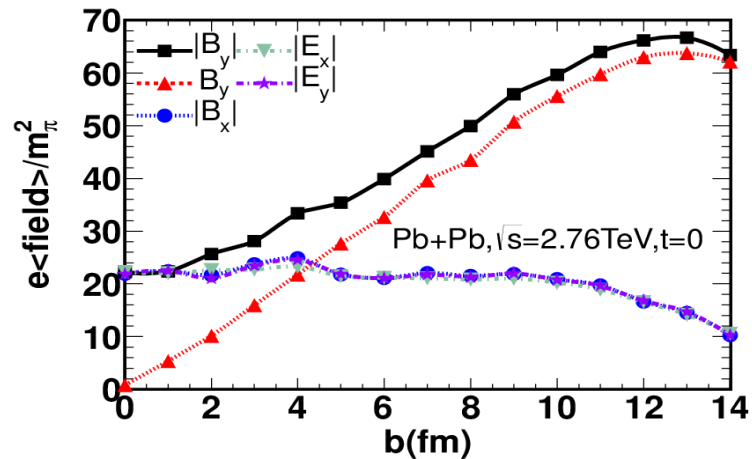
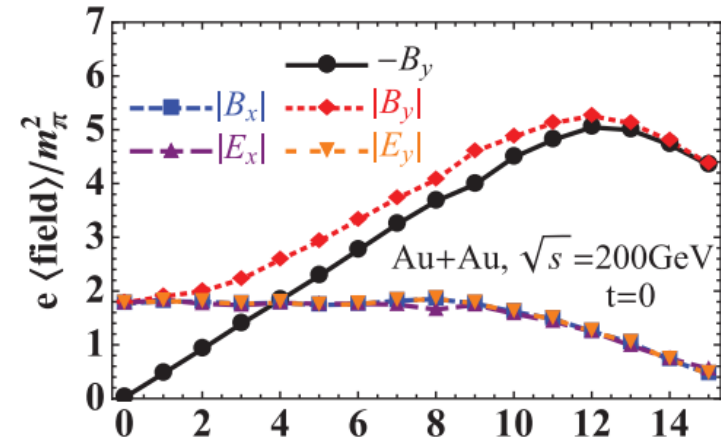
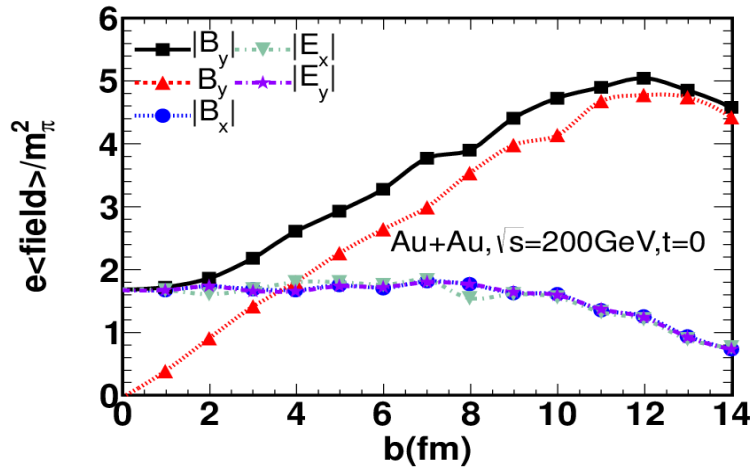
$$\Psi_2 = \Psi_{EP}$$

Introduction : string-melting AMPT model



2 Numerical results and discussions

EM fields in AuAu, PbPb collisions

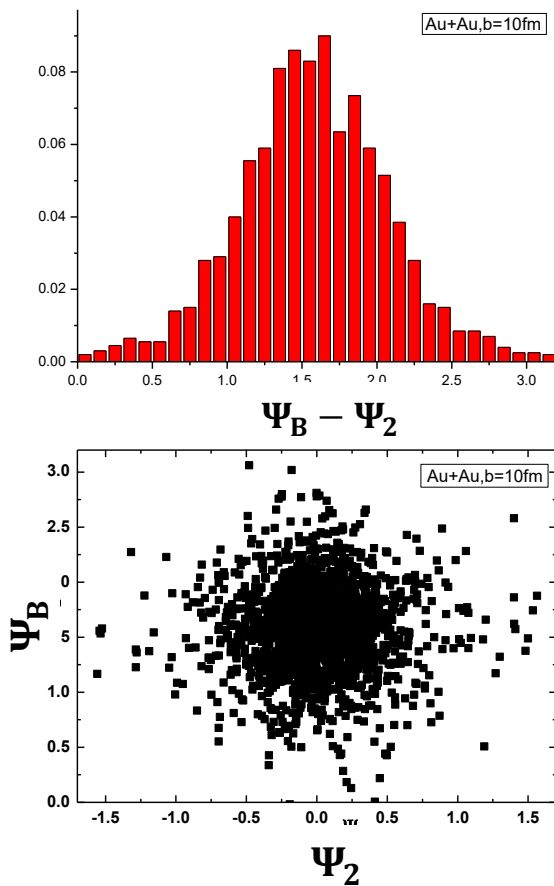


our results

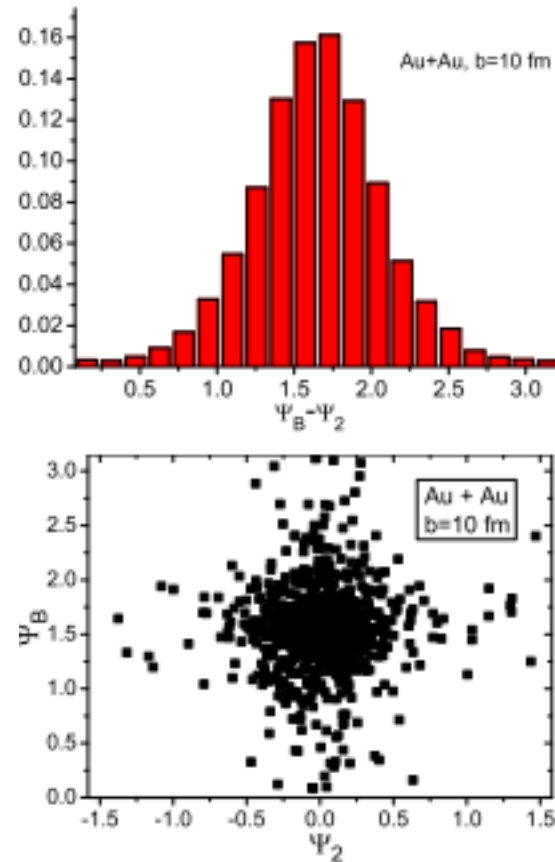
W. T. Deng and X. G. Huang, Phys. Rev. C 85, 044907 (2012)

The results are almost the same.

Ψ_B and Ψ_2 in $\sqrt{S} = 200\text{GeV}$ AuAu collisions



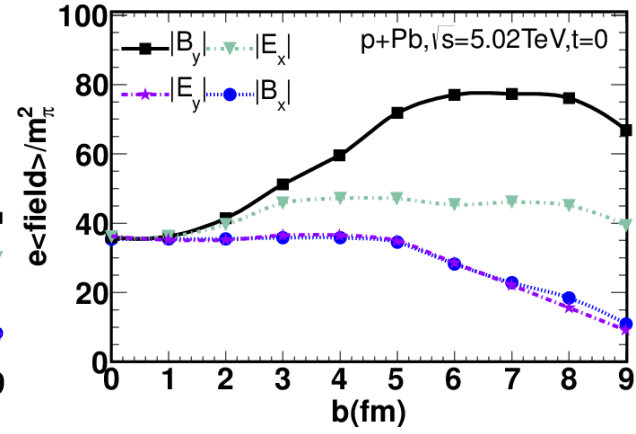
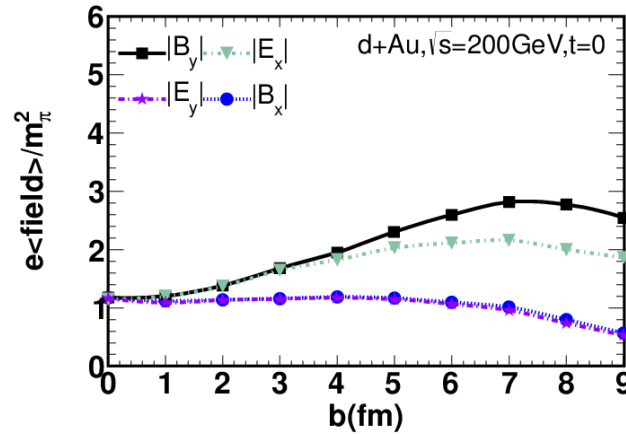
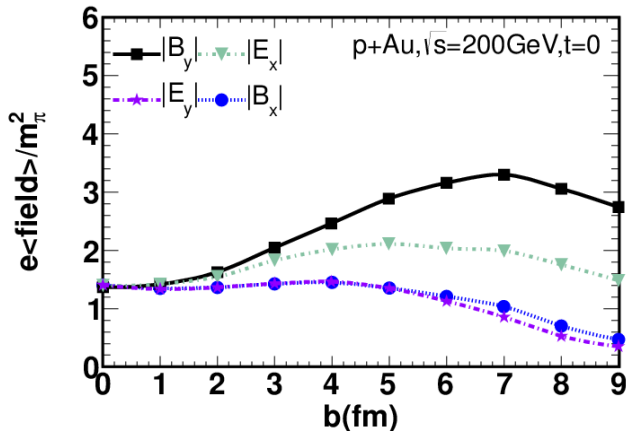
our results



John Błoczyński, X.G Huang et al, arXiv:1209.6594v2

The results are almost the same.

EM fields in pAu , dAu , pPb collisions

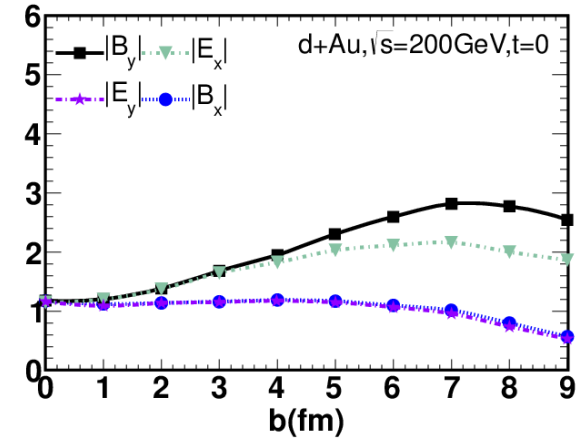
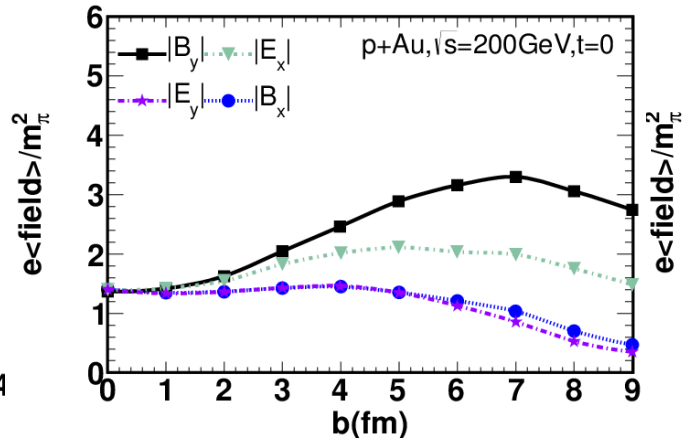
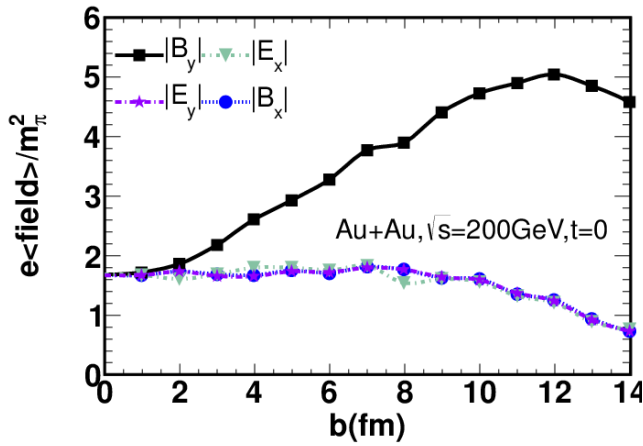


$$\frac{|B_{pPb}|}{|B_{pAu}|} \approx \frac{|B_{pPb}|}{|B_{dAu}|} \approx 25$$

$$\frac{5020\text{GeV}}{200\text{GeV}} \approx 25$$

$$B \propto \sqrt{s}$$

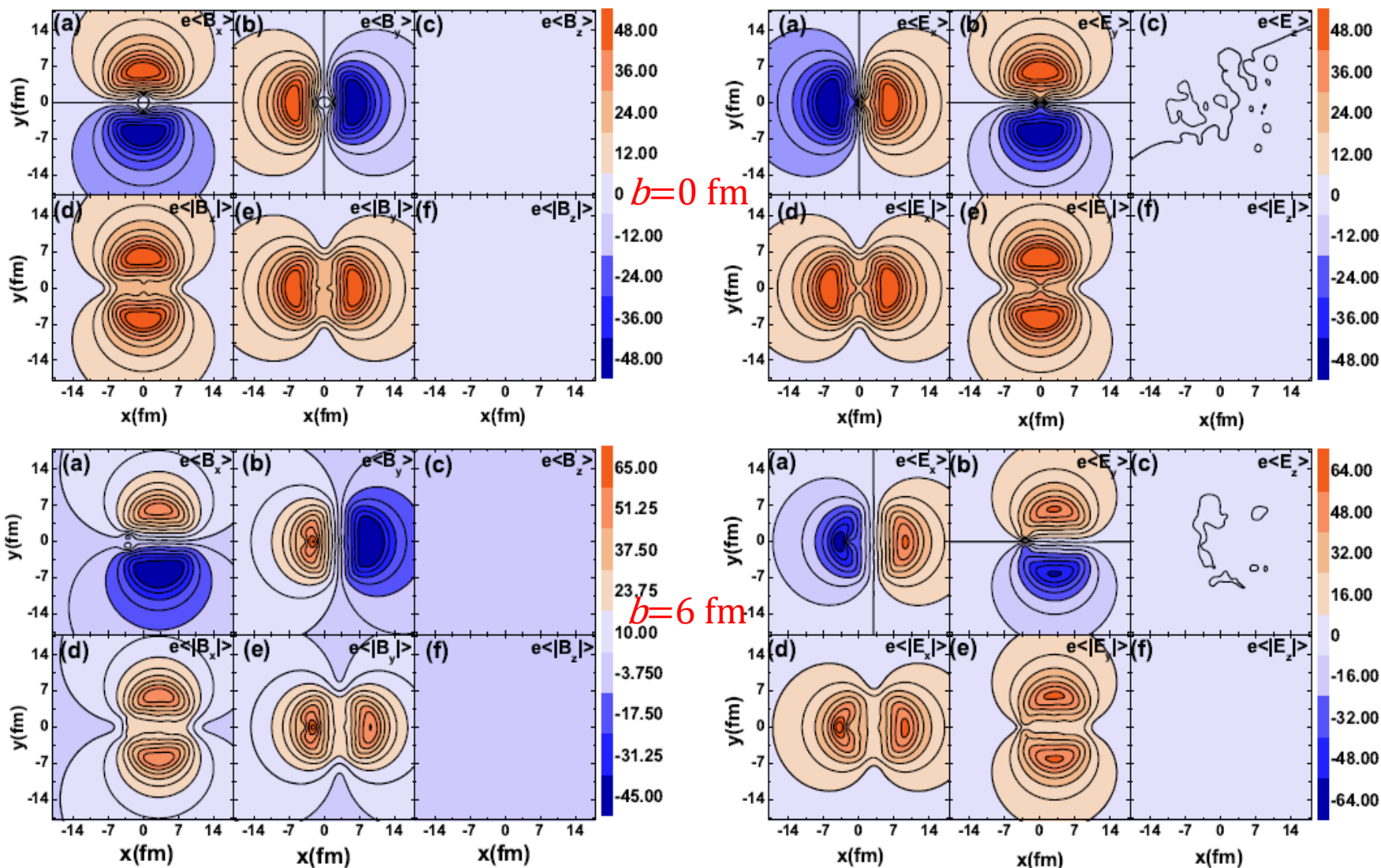
EM fields in AuAu, pAu, dAu collisions



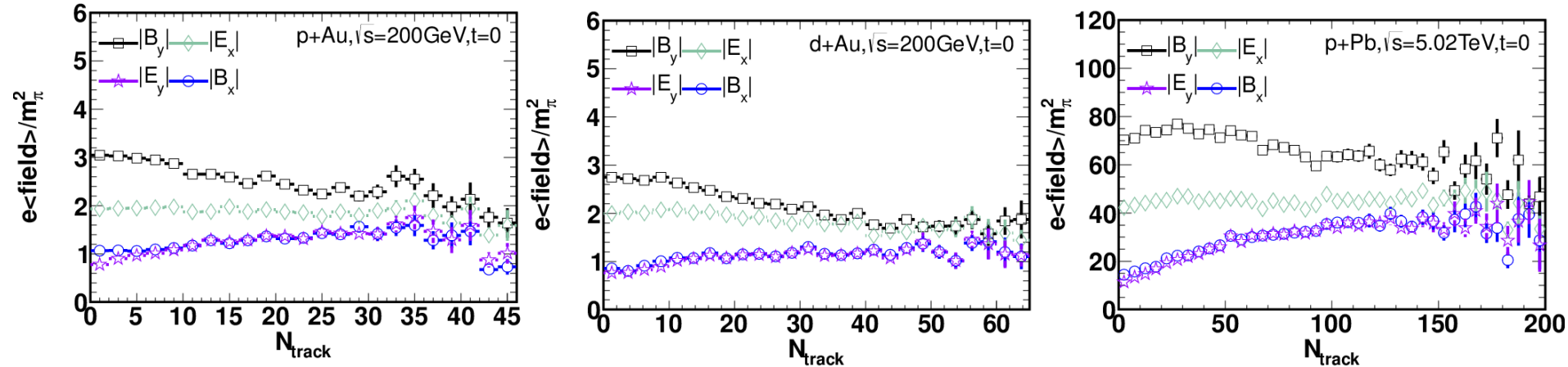
$$\frac{|B_{AuAu}|}{|B_{pAu}|} \approx \frac{|B_{AuAu}|}{|B_{dAu}|} \approx 2$$

$$B \propto Z$$

Spatial distribution of EM fields in $\sqrt{S} = 5.02 TeV$ pPb collisions



EM fields in pAu , dAu , pPb collisions



$$\Delta r \propto \sqrt{\langle B^2 \cos 2(\Psi_B - \Psi_2) \rangle}$$

✓
???

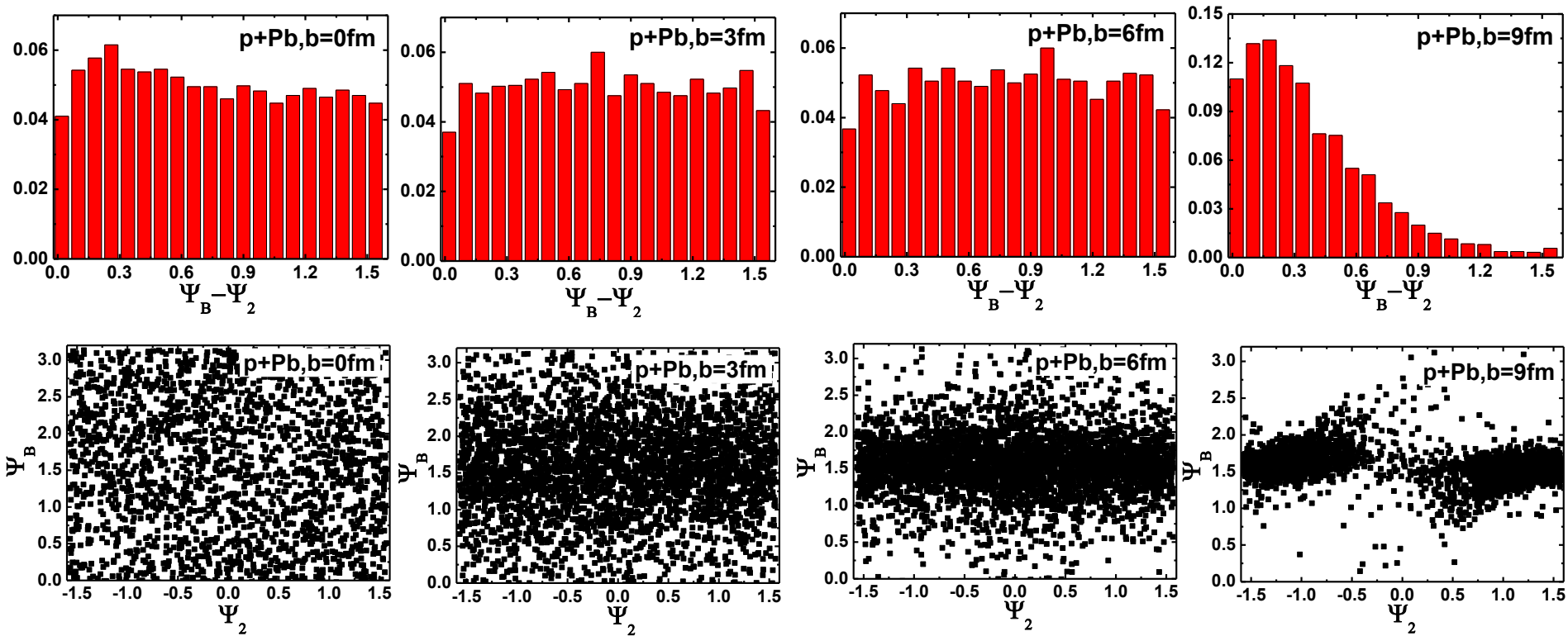
N_{track} is the number of charged particles after collisions.

The definitions of N_{track} are the same to the experiments.

RHIC energy: $|\eta| < 2.4$ & $P_T > 0.4 \text{ GeV}$

LHC energy: $|\eta| < 1$ & $P_T > 0.15 \text{ GeV}$

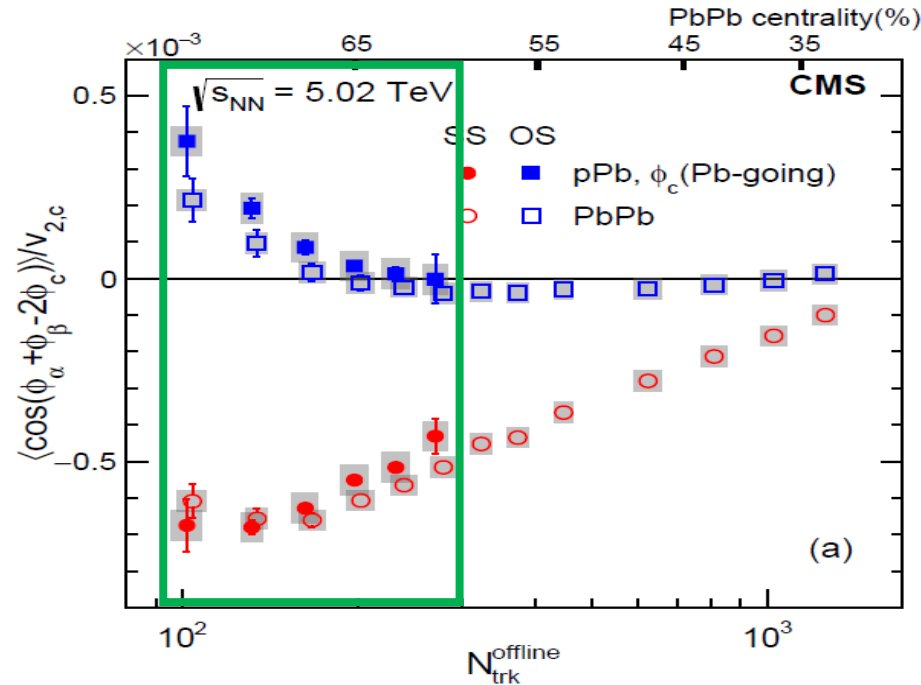
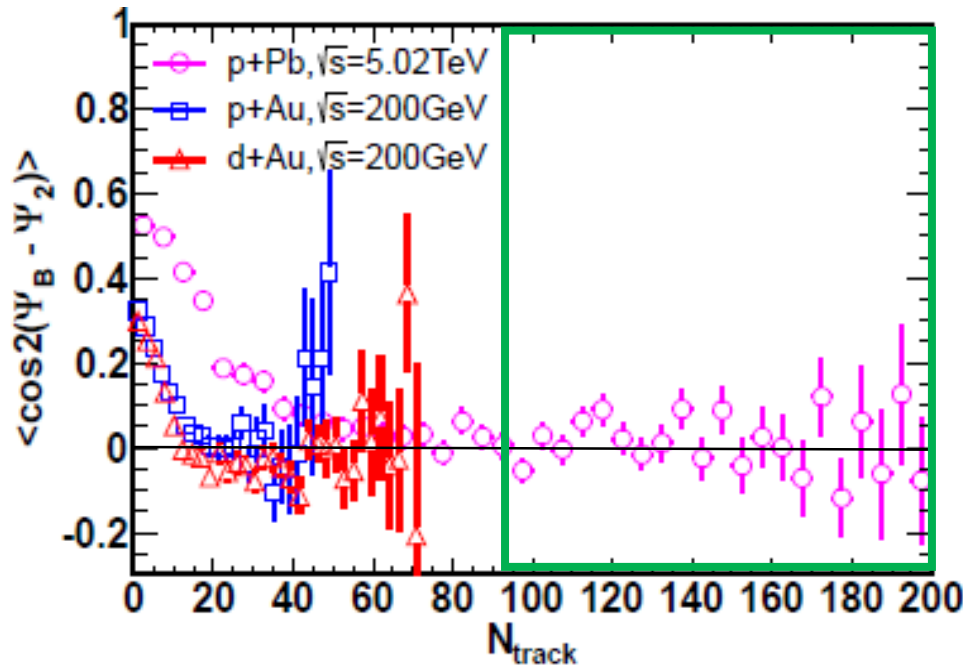
Ψ_B and Ψ_2 in pPb collisions at $\sqrt{S} = 5.02 TeV$



Going from $b = 3$ to 6 fm, $\Psi_B \rightarrow \frac{\pi}{2}$, but Ψ_2 is always random.

In very peripheral collisions (last figure), Ψ_2 is special because the number of partons is less and they can't define Ψ_2 very well.

$\langle \cos 2(\Psi_B - \Psi_2) \rangle$ in pAu , dAu , pPb collisions



For high-multiplicity events, $\langle \cos 2(\Psi_B - \Psi_2) \rangle \approx 0 \Rightarrow \Delta\gamma^{\text{CME}} \approx 0$.

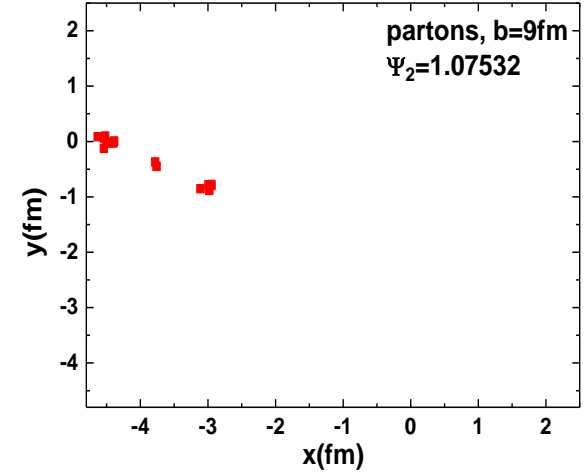
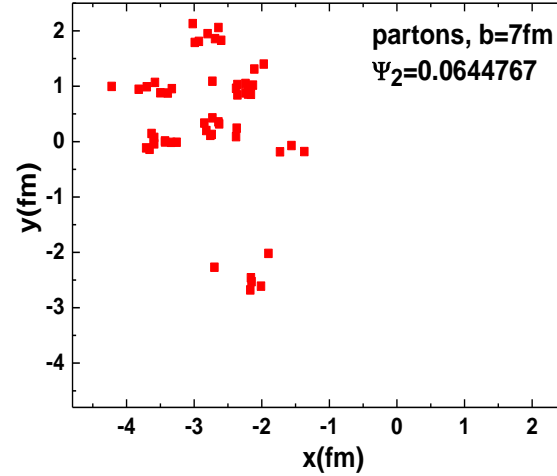
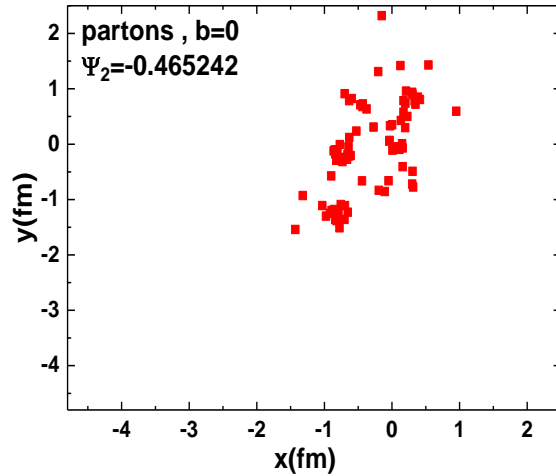
Summary

Using AMPT, we studied :

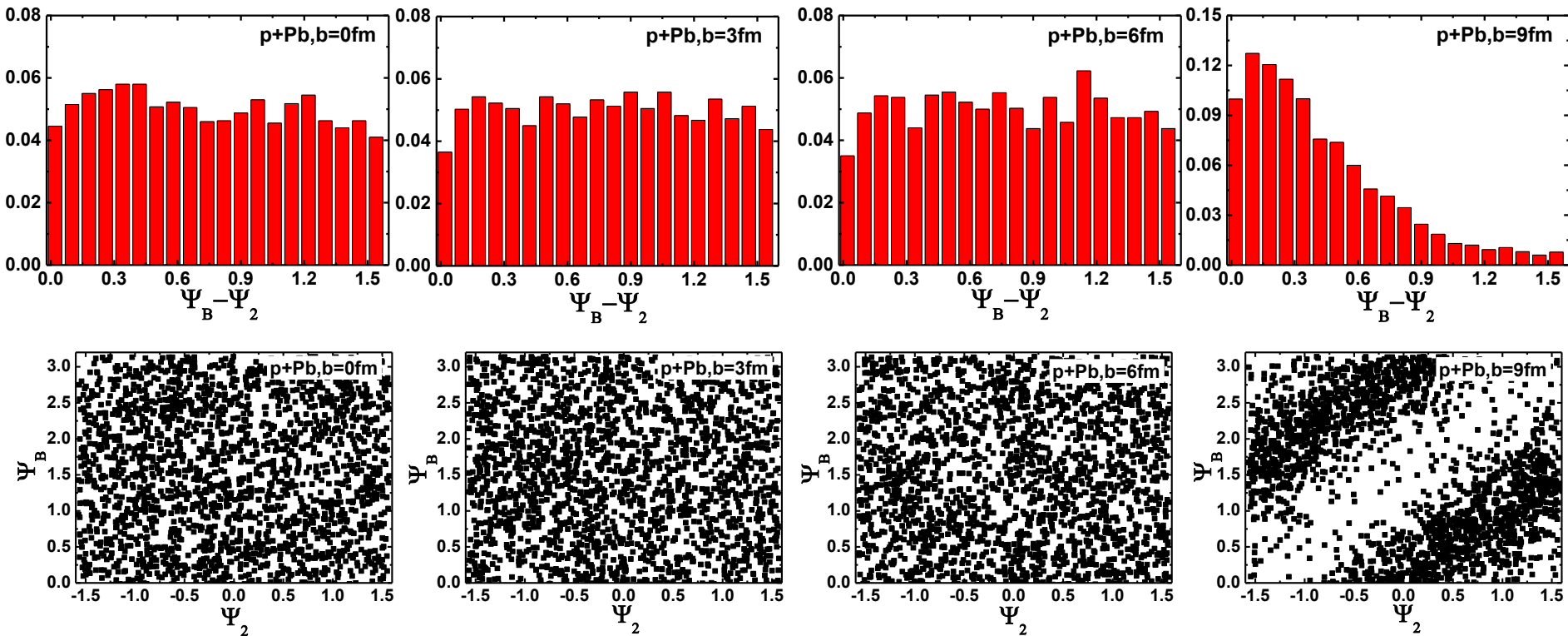
- ◆ the relationships between EM fields and b, N_{track} .
- ◆ the spatial distributions of the EM fields.
- ◆ in pAu, dAu, pPb collisions, $\langle \cos 2(\Psi_B - \Psi_2) \rangle \approx 0$ for high-multiplicity events. This indicates that the traditional experimental CME observable three-particle correlation is not sensitive to CME any more for small systems.

Thank you for
your attention!

The distributions of partons and Ψ_2 in different centrality

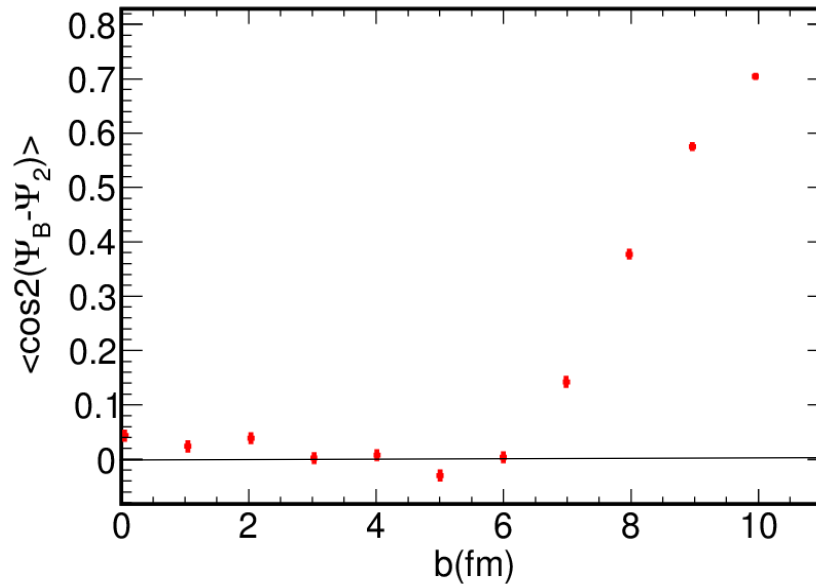


Ψ_B and Ψ_2 in $\sqrt{S} = 5.02 \text{ TeV}$ pPb collisions, random orientation of reaction plane in AMPT



Ψ_B & Ψ_2 are all random.

$\langle \cos 2(\Psi_B - \Psi_2) \rangle$ in $\sqrt{S} = 5.02 \text{ TeV } p\text{Pb}$ collisions random orientation of reaction plane in AMPT



The results of $\langle \cos 2(\Psi_B - \Psi_2) \rangle$ are similar to previous calculations.

This is because the rotation of the coordinate system does not affect the results of $\Psi_B - \Psi_2$.

The definitions of Ψ_B and Ψ_2

$$\Psi_2 = \frac{\text{atan2}(\langle r^2 \sin(2\phi) \rangle, \langle r^2 \cos(2\phi) \rangle) + \pi}{2}$$

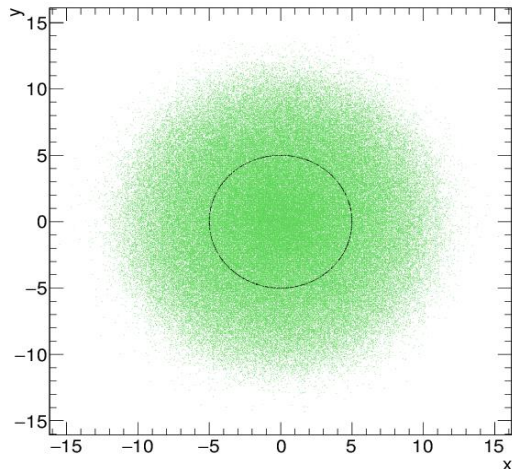
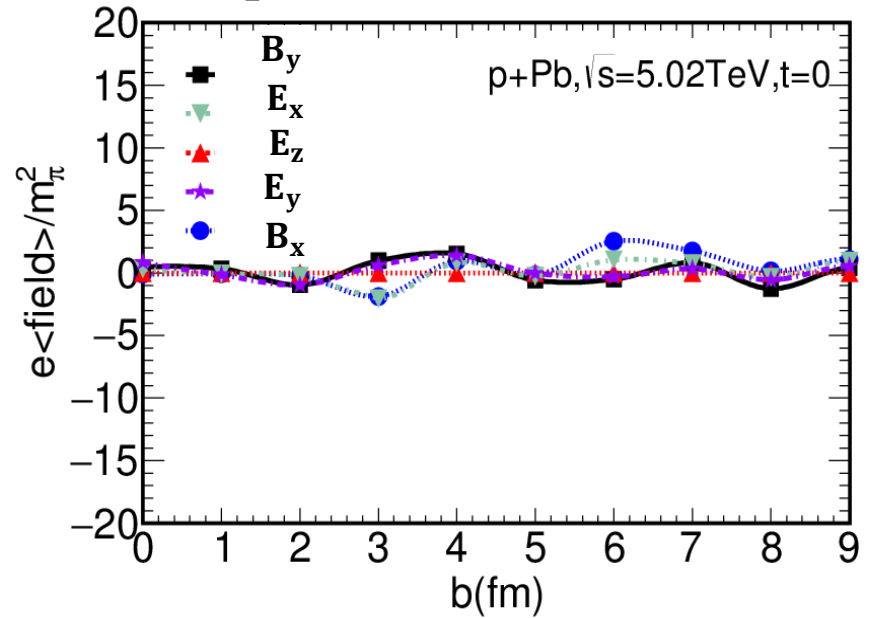
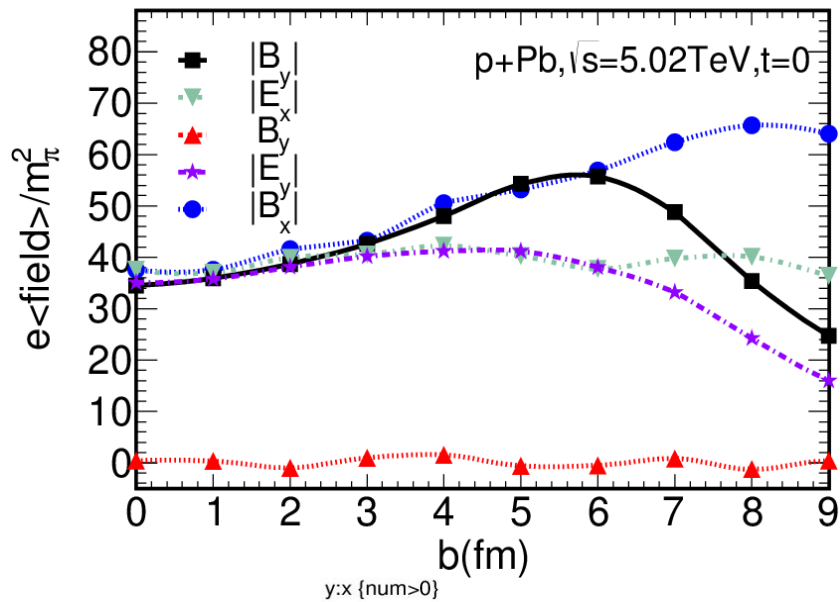
$$\Psi_B = \text{atan2}(B_y, B_x)$$

$$\Psi_B \in (-\pi, \pi), \Psi_2 \in (-\pi, \pi)$$

$$\text{or } \Psi_B \in (-\pi, \pi), \Psi_2 \in \left(-\frac{\pi}{2}, \frac{\pi}{2}\right)$$

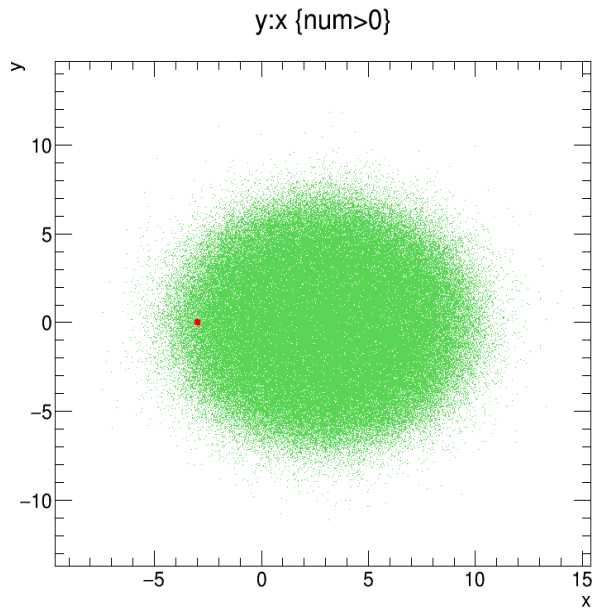
EM fields in $\sqrt{S} = 5.02\text{TeV}$ pPb collisions

random orientation of reaction plane in AMPT

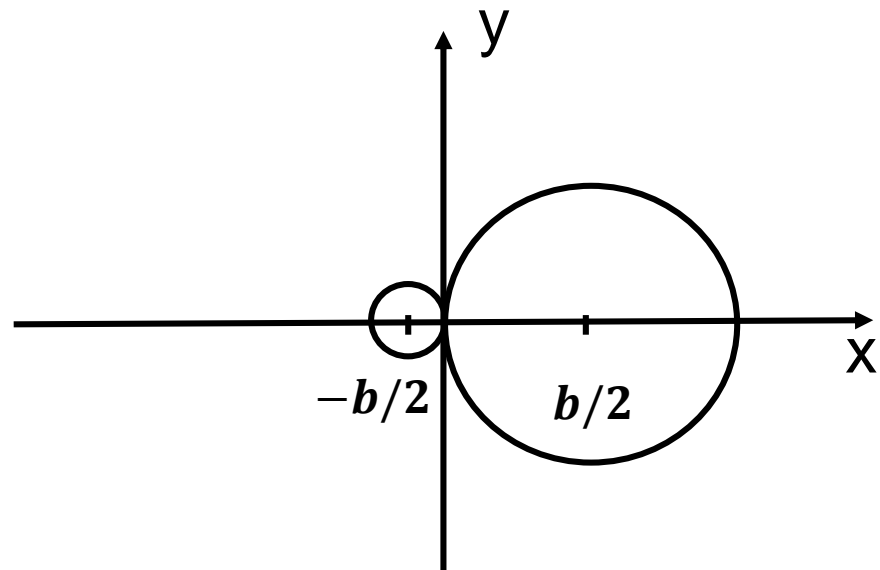


green dots are the nucleons of Pb
black dots are the nucleons of p

Geometry of particular events in small systems



green dots are the nucleons of Pb
red dots are the nucleons of p



Geometry in AA collisions

The geometric image:

